Journal of Glaciology, Vol. 12, No. 65, 1973

SHORT-TERM SNOW MELT AND ABLATION DERIVED FROM HEAT- AND MASS-BALANCE MEASUREMENTS

By PAUL M. B. FÖHN*

(Department of the Environment, Inland Waters Branch, Ottawa, Ontario, Canada)

ABSTRACT. The daily snow melt calculated from meteorological observations is compared with detailed mass-balance measurements taking into account internal changes in density and free water content in the surface layers of a glacier snow-pack. The energy balance is calculated from measurements obtained by a meteorological station at the experimental site. In addition to the standard ablation measurements the run-off from the melting snow-pack was obtained for a few days. The snow-density profiles were measured with a portable gamma-transmission probe and the liquid-water content of snow was determined by a calorimetric method.

Agreement between the melt calculated by the heat-balance method and the mass changes observed in the mass-balance measurements is fair for daily periods. It appears that about 20% of the daily snow melt takes place internally as a result of penetration of solar radiation.

RÉSUMÉ. *Étude de la fonte et de l'ablation de la neige à partir de mesures du bilan thermique et du bilan de masse, effectuées pendant une courte période de temps.* La fonte journalière de neige calculée à partir d'observations météorologiques est comparée à des mesures détaillées de bilan de masse. Cette comparaison tient compte des variations internes de densité et de volume d'eau libre se produisant dans les couches superficielles du névé d'un glacier. Le bilan énergétique est calculé à partir de mesures fournies par une station météorologique, située sur le site expérimental. En plus des mesures standard d'ablation, le ruissellement résultant de la fonte de neige a été aussi calculé pour une période de quelques jours. Les profils de densité de la neige ont été effectués à l'aide d'une sonde portative de transmission gamma. Le volume d'eau libre contenu dans la neige a été déterminé par une méthode calorimétrique. Sur une base journalière, on peut dire que l'accord entre le taux de fonte calculé à partir du bilan thermique et celui obtenu à partir des variations observées dans le bilan de masse, est acceptable. Il semble qu'environ 20% de la fonte journalière de neige se produisent en profondeur comme résultat de la pénétration des radiations solaires.

ZUSAMMENFASSUNG. *Bestimmung kurzfristiger Schmelz- und Ablationsbeträge mit Hilfe von Wärme- und Massenbilanzmessungen.* Die aus meteorologischen Beobachtungen berechneten Tagesraten der Schneeschmelze werden mit detaillierten Massenbilanzmessungen verglichen, die interne Dichteänderungen und den Gehalt freien Wassers in den Oberflächenschichten einer Gletscherschneedecke berücksichtigen. Die Energiebilanz wurde aus Messungen berechnet, die an einer meteorologischen Station im Versuchsfeld ausgeführt wurden. Zusätzlich zu den üblichen Ablationsmessungen erhielt man den Abfluss einer schmelzenden Schneedecke für wenige Tage. Die Schneedichteprofile wurden mit einer transportablen Gammasonde aufgenommen; der Wassergehalt des Schnees wurde mit Hilfe einer kalorimetrischen Methode bestimmt. Die Übereinstimmung zwischen den Schmelzbeträgen, die mit Hilfe der Wärmebilanz berechnet wurden, und den beobachteten Massenänderungen bei den Massenbilanzmessungen ist für die täglichen Werte befriedigend. Es zeigt sich, dass etwa 20% der täglichen Schneeschmelze im Innern stattfindet, was auf das Eindringen der Sonnenstrahlung zurückzuführen ist.

INTRODUCTION

Combined heat- and mass-balance studies provide, besides the insight into the transfer processes between atmosphere and ground, a potentially simple tool for indirect evaluation of melt and ablation rates. This implies that the adequacy of the transfer equations as well as the reliability of the collected heat-balance data must be checked against independent direct evaluations of melt and ablation rates, at least during a certain "assessment" period.

During a short summer period of 1970 detailed measuring procedures were determined for short-term snow melt and ablation rates. The study was carried out as a first step in a series of investigations dealing with the mechanisms of mass and energy transfer to and in a snow-pack.

The concrete questions were:

Is it possible to measure directly melt and ablation rates of a glacier snow-pack with sufficient accuracy for short time intervals?

* Present address: Eidg. Institut für Schnee- und Lawinenforschung, 7260 Weissfluhjoch/Davos, Switzerland.

How well do melt rates, obtained as residuals in a heat balance equation, compare with the former ones, if only data from extended standard meteorological equipment ([International Hydrological Decade], 1970) are available, i.e. certain commonly measured quantities have to be replaced by estimates?

The observations were made at an experimental site, at this time still snow-covered, located in the upper ablation area of Peyto Glacier, Alberta, Canada (lat. 51° 39′ 40″ N., long. 116° 33′ W., elevation 2 510 m a.s.l.) during the period 1 to 15 July 1970. The site was chosen in the centre of a nearly level plateau (slope 2°). It was equipped with a net radiometer (for a short description of instruments see the Appendix), a continuously recording meteorological station, an ablatometer, and a gamma transmission probe for continuous snow density profiles. Additional equipment consisted of a pyranograph, a precipitation gauge, evaporation pans, a small snow-melt lysimeter and equipment to measure snow density and liquid-water content of small snow samples.

Theory and measurements

Mass balance. Limiting the discussion to a melting snow-pack, particularly to a snow column in the uppermost layers of a temperate glacier, the ablation A, for a period with no precipitation, may be expressed by a combined ice and water balance equation as:

$$A = R \pm E \pm W = SM \pm DM \pm E \pm W \qquad (1)$$

where A, the ablation, is the total loss of water in all phases, R is the run-off, E is the water-vapour exchange at the surface, W is the mass exchange by wind action, SM is the snow-melt, and DM is the sub-surface mass change due to storage changes of liquid water. In contrast to the internal mass changes in the pack, the wind action and the vapour exchange at the surface are often negligible quantities for short intervals. The internal mass changes are mainly dependent on the liquid water movement in the pack. For a highly porous, inhomogeneous and unsaturated material like snow, the water movement is controlled, among other things, by the melt intensity. Thus, the snow moisture content changes during the day as the melt intensity does.

Hubley (1954) formulated an expression for the ablation which takes care of these changes and presented all quantities involved as functions of time:

$$\frac{\mathrm{d}M}{\mathrm{d}t} = \rho_{ih}\frac{\partial h}{\partial t} \pm \int_0^h \frac{\partial \rho_i}{\partial t}\,\mathrm{d}z \pm \rho_{wh}\frac{\partial h}{\partial t} \pm \int_0^h \frac{\partial \rho_w}{\partial t}\,\mathrm{d}z. \qquad (2)$$

M denotes the total mass of a snow column of height h, z is the vertical co-ordinate, ρ_i the "dry" snow density or the density of the ice matrix and ρ_w is the volume fraction of the total snow density (ρ_s) due to the presence of liquid water. The subscript h indicates the reference location of the terms, in this case a small surface layer. The first two terms on the right in Equation (2) express under the given conditions the melt and compaction in the snow-pack, whereas the next two terms account for the changes in liquid-water storage. This separation of the snow-pack into a solid and a liquid phase (the vapour phase is negligible within the pack under isothermal conditions) and into two zones (surface and sub-surface zone) allows the calculation of melt rates. Heat balance calculations yield melt rates, not ablation rates, therefore measured melt rates are of primary interest whenever a comparison with such calculated quantities is desirable. In addition, melt rates can be evaluated by controlling only the surface layers of a snow-pack, because snow-melt processes are confined to the top 0.3 m of a ripe pack. For the evaluation of ablation rates, the whole snow column extending to an impermeable layer, where the outflow of the water takes place, has to be surveyed. As shown later in this study, the build-up and the fluctuations of a water table on top of an impermeable layer (old ice surface) can significantly influence measured ablation rates.

Assuming that the compaction of the snow-pack can be neglected for short intervals (Ambach and Hoinkes, 1963, reported for similar conditions a mean value of 2 mm per day), the first two terms of Equation (2) can be integrated. The melt in the interval $(t_1 - t_0)$ is then given by:

$$SM = \rho_{i\Delta h}(t_0)\,\Delta h + [\rho_{i\Delta h'}(t_0) - \rho_{i\Delta h'}(t_1)]\,\Delta h' \qquad (3)$$

where $\rho_{i\Delta h}(t_0)$ is the initial mean ice density of the surface layer (thickness $= \Delta h$) and $\rho_{i\Delta h'}(t_0)$, and $\rho_{i\Delta h'}(t_1)$ are the mean ice densities of the lower layers (thickness $= \Delta h'$), which are affected by melt, at the beginning and the end of the interval respectively. The various depth intervals are displayed in Figure 1.

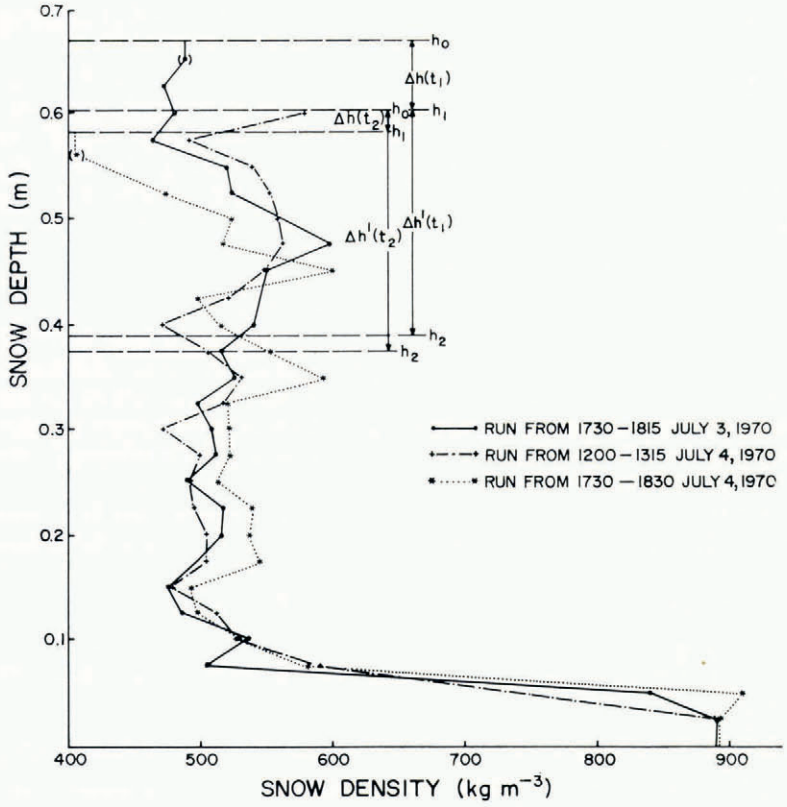

Fig. 1. Snow density profiles at different times, measured with a gamma transmission probe. Values in brackets were obtained gravimetrically as the top layer at the probe location was sometimes influenced by additional melt from the installations.

The ice density values ($\rho_i = \rho_s - \rho_w$) were calculated by using continuous snow-density profiles (gamma transmission probe) and liquid-water content measurements. The surface lowering Δh was estimated by means of successive surface lowering readings with an ablatometer. The surface lowering and the density measurements were performed at the same location. There is, however, no technique to measure *in situ* changes of liquid-water content of snow. Consequently, the liquid water content was obtained by repeated sampling of the layers, using the freezing calorimetric method (Radok and others, 1961).

$\Delta h'$ was estimated by using the Bouger–Lambert law:

$$I_z = I_0 \exp(-\nu z) \qquad (4)$$

https://doi.org/10.3189/S0022143000032093 Published online by Cambridge University Press

where I_z is the hourly net short-wave radiation intensity at level $z = h_2$, I_0 is the maximum hourly net short-wave radiation intensity per interval at the minimum surface level $z = h_1$. The extinction coefficient, ν, was assumed to be 1.8 mm^{-1} for this wet and ripe snow (Mellor, 1964). The net short-wave radiation has been determined by means of the measured short-wave radiation and with mean values of albedo deduced from measurements by Miller (1950). By assigning to I_z a small value of 33.4 kJ m^{-2} h^{-1} which produces the negligible melt of 0.1 mm of water per hour, the maximum melt-layer thickness $\Delta h' = h_1 - h_2$ can be calculated for each interval:

$$\Delta h' = \frac{1}{\nu} \ln \frac{I_z}{I_0}. \tag{5}$$

This thickness varied in a range from 0.14 to 0.22 m during the period of continuous snow cover.

Since it is common practice in combined heat- and mass-balance studies to compare the heat input with measured ablation rates, the ablation rates were evaluated too. Various techniques reported by LaChapelle (1959) and Müller and Keeler (1969) were used to measure these ablation rates. The first one consisted in measuring directly the mass loss of adjacent snow columns in time down to the impermeable, "superimposed-ice" surface.

The ablation A was calculated from

$$A = \int_0^{h_0} \rho_s(z, t_0)\, dz - \int_0^{h_0} \rho_s(z, t_1)\, dz \tag{6}$$

where $\rho_s(z, t_0)$ and $\rho_s(z, t_1)$ represent the total snow density profiles at time t_0 and t_1 respectively. These successive density profiles were obtained with the aid of the gamma transmission probe. Unfortunately the method could not be applied to the whole observation period, because the installations caused additional melt and influenced the measurements appreciably toward the end of the period.

The second method which could not be performed at the same location but was feasible for the whole period was to sample snow or ice cores with respect to a stable reference horizon according to:

$$A = \bar{\rho}_s(t_0)\, h_0 - \bar{\rho}_s(t_1)\, h_1 \tag{7}$$

where $\bar{\rho}_s$ is the average snow density of the cores.

The third method was based on measurement of the surface lowering for each interval and on the initially measured average density.

$$A = \bar{\rho}_s(t_0)[h_0 - h_1]. \tag{8}$$

All melt and ablation rates were evaluated daily for two successive periods with supposedly similar melt amounts. A six-hour afternoon period (12.00 h to 18.00 h) and an eighteen-hour night/morning period (18.00 h to 12.00 h) fulfilled this condition satisfactorily and permitted measurements at convenient times.

To obtain an additional independent measurement for the ablation rate of the snow-pack, at least for a part of the period, a provisional snow-melt lysimeter was installed at the site (Fig. 2). For this purpose a snow block of 0.5 m^2 surface area was separated by vertical trenches from the remaining pack. At the lower boundary and along the smooth "superimposed-ice" surface, an additional thin snow layer was gradually removed from three sides for about two-thirds of the area. Before the remaining part of this layer was removed, a large transparent plastic sheet was positioned at this lower, now accessible boundary. By pushing the snow block forward towards the spread sheet the whole block was brought to the centre of the sheet. The side parts of the sheet were then taken up along the walls. The enclosed block was brought back into its original position in the snow-pack, so that only one small corner,

where the outlet was installed, was not surrounded by the snow-pack. At day-time the melt-water outflow from this block was collected over intervals of $\frac{1}{2}$ to 2 h in a large container and the volume measured with a graduated cylinder. During the night the small outflow was similarly collected and measured the following morning. Although no continuously recording system could be established for this trial and therefore no continuous outflow curve could be obtained, the total daily outflow could be measured for a few days (cf. values of last column in Table III).

Fig. 2. Provisional snow-melt lysimeter and snow surface conditions.

In order to get another independent check for the heat-balance equations in addition to the residual melt, Q_{SM} (Equation (9)), direct evaporation measurements were made. The net evaporative loss was determined by weighing three circular, snow-filled plastic pans at the beginning and end of each interval. The pans were about 20 cm deep, had a surface area of 450 cm^2 and were refilled with surface snow without destroying its surface features and structure. Natural conditions were assured by placing these pans in the snow-pack so that their top rim was flush with the surrounding snow surface. The results of these measurements are represented in the last column of Table 1.

Heat balance. Any heat-balance calculation may be subject to systematic errors, because most of the transfer equations are empirical and the theoretical framework is still not sufficient for the range of atmospheric stabilities experienced. Keeping this and the instrumental limitations of this study in mind, the observation period and the site were selected in such a way that only four quantities had to be considered. The heat available for melting, Q_{SM}, could be represented by:

$$Q_{SM} = Q_R \pm Q_H \pm Q_E \qquad (9)$$

https://doi.org/10.3189/S0022143000032093 Published online by Cambridge University Press

where Q_R is the net radiation, Q_H the sensible heat component and Q_E the latent heat component.

A brief outline of the heat balance theory usually applied explains the specific conditions and the necessary assumptions. The net all-wave radiation was measured directly with a net radiometer. The transfer of heat and water vapour was estimated by means of theories,

TABLE I. MEAN VALUES OF AIR TEMPERATURE, WATER VAPOUR PRESSURE, WIND SPEED AND CLOUD AMOUNT FOR A 6 h (A) AND 18 h (B) PERIOD FOR EVERY 24 h INTERVAL. THE TOTALS OF NET ALL-WAVE AND SHORT-WAVE RADIATION AND THE TOTALS OF THE CALCULATED AND MEASURED MELT AND EVAPORATION/CONDENSATION RATES ARE ALSO REPRESENTED FOR THE SAME PERIODS

Date		*Air temperature*	*Water vapour pressure*	*Wind speed*	*Cloud amount*	*Net all-wave radiation*	*Short-wave radiation*	*Calculated melt* (SM_{C1})	*Measured melt* (SM_M)	*Calculated evap./cond.*	*Measured evap./cond.*
July 1970	*Period*	°C	mb	m s^{-1}	tenths	KJ m^{-2}	KJ m^{-2}	mm	mm	mm	mm
1*	A	4.2	5.4	3.8	7	1 940	16 153	8.6	11.9	−0.13	−0.10
	B	4.0	5.2	1.7	4	−1 005	12 108	0.1	14.3	−0.22	−0.28
2	A	7.9	6.3	1.7	5	2 820	14 444	12.2	20.0	0.01	−0.30
	B	6.7	7.0	2.8	3	373	15 022	20.9	23.4	0.36	0.17
3	A	8.6	7.5	3.4	2	3 617	18 212	21.7	34.4	0.22	0.33
	B	9.9	8.2	3.6	3	553	12 183	41.7	29.0	0.95	0.53
4	A	11.5	8.6	2.3	5	4 296	14 821	23.5	15.0	0.26	0.13
	B	9.3	8.0	2.6	3	2 989	6 820	36.4	38.8	0.70	0.33
5	A	11.4	6.2	2.5	3	4 999	18 891	22.6	32.8	0.01	−0.16
	B	9.0	6.0	2.2	1	3 090	13 808	24.2	24.2	−0.04	−0.37
6	A	10.3	6.6	2.2	4	4 120	16 052	18.9	15.8	0.05	−0.13
	B	8.6	7.1	3.0	3	2 512	13 029	33.5	28.5	0.43	0.56
7	A	13.0	7.8	2.5	2	5 100	18 112	26.5	21.3	0.20	0.17
	B	12.0	8.3	2.6	2	3 015	15 223	44.1	49.4	0.79	0.21
8	A	13.5	6.7	2.0	3	4 296	17 685	20.6	16.5	0.05	−0.13
	B	10.3	5.8	2.8	3	2 487	13 339	27.7	29.3	−0.13	−0.52
9	A	10.9	6.4	2.5	3	5 476	16 756	23.5	16.3	0.03	−0.01
	B	8.7	6.5	3.8	3	2 006	13 590	32.9	34.7	0.20	0.55
10	A	10.3	6.5	3.1	5	5 552	15 474	26.2	31.1	0.06	0.18
	B	8.1	6.6	2.0	3	1 080	11 606	20.6	13.4	0.17	—
11	A	6.4	6.1	2.4	7	1 608	9 546	10.0	8.4	0.0	—
	B	4.0	6.3	2.6	8	1 407	4 044	4.6	0.9	0.07	—
12	A	2.2	5.5	1.5	8	2 487	10 760	7.6	15.2	−0.03	—
	B	2.2	5.1	1.9	3	5 979	15 299	17.7	6.3	−0.17	—
13	A	5.1	4.8	1.5	2	10 551	19 820	32.2	22.4	−0.06	—
	B	5.7	4.9	2.3	4	4 913	13 967	17.6	40.3	−0.24	−1.08
14	A	5.8	5.5	2.8	4	8 868	16 153	28.1	21.2	−0.05	−0.24
	B	7.6	5.9	2.1	2	4 277	13 766	19.0	22.0	−0.04	−0.92
Total period	A					65 730	222 879	282.2	282.3	+0.62	
Mean value period	A	8.65	6.40	2.42	4.4						
Total period	B					30 861	173 804	341.0	354.5	+2.83	
Mean value period	B	7.58	6.48	2.56	3.2						
Total for the whole period						96 591	396 683	623.2	636.8	+3.45	
Mean value for the whole period		7.85	6.46	2.53	3.5						

* The values presented for a certain day j are actually the values calculated or measured from 12.00 h of day j to 12.00 h of day $j+1$.

https://doi.org/10.3189/S0022143000032093 Published online by Cambridge University Press

mainly developed by Prandtl and Taylor (cf. Brunt, 1952). According to these the sensible heat flux F_H may be calculated from:

$$F_H = -\rho_a C_p K_H \left(\frac{\partial T}{\partial z} + \Gamma\right) \tag{10}$$

where z is the vertical co-ordinate with its origin at the surface, T the absolute air temperature, Γ the dry adiabatic lapse rate, and C_p the specific heat of air at constant pressure, ρ_a is the density of air and K_H the coefficient of eddy diffusivity. Similarly for the latent heat flux F_E:

$$F_E = -\rho_a K_E \frac{\partial q}{\partial z} \tag{11}$$

where q denotes the specific humidity and K_E the coefficient of eddy diffusion of water vapour. Finally the effect of the turbulent air motion on the transfer process can be described by:

$$\tau = \rho_a K_M \frac{\partial u}{\partial z} \tag{12}$$

where τ is the mean shear stress, u a mean value of the horizontal component of the eddy velocity and K_M the eddy viscosity of air. It may be noted that the vertical wind component is assumed to be proportional to, and of the same order of magnitude as, u.

The usual procedure is now to evaluate the coefficient K_M using wind profile data and assumptions for the exchange-layer thickness, the stability of the atmosphere and the vertical distribution of the shear stress. However, because of its simplicity, many investigators make use of von Kármán's logarithmic equation for the wind velocity distribution, even so they dispose, e.g., of detailed wind profile data, which may indicate quite irregular wind profiles. This equation was derived for an adiabatic atmosphere and can be written in the form:

$$u = \frac{1}{k}\left[\frac{\tau_0}{\rho_a}\right]^{\frac{1}{2}} \ln \frac{z+z_0}{z_0} \tag{13}$$

where k is the dimensionless von Kármán constant, τ_0 the shear stress at the lower atmospheric boundary and z_0 the surface roughness parameter, a height where the wind velocity is zero. If the shear stress does not change appreciably with the vertical distance z ($\tau \approx \tau_0$), an assumption which was confirmed by recent investigations of Haugen and others (1971), Equations (12) and (13) may be combined and K_M can be calculated from

$$K_M = \frac{k^2 u_1 (z_1+z_0)}{\ln\left[(z_1+z_0)/z_0\right]} \tag{14}$$

where u_1 is the mean horizontal wind velocity at height z_1. Assuming, additionally, that the eddy diffusivity coefficients are identical for the transfer of momentum, heat and vapour, and assuming that the eddy diffusivity coefficients are constant with height, the different fluxes may be calculated.

Grainger and Lister (1966) compared different relations describing the wind distribution over cold surfaces and concluded that a simple logarithmic law is most applicable over a wide range of stability conditions. This conclusion and the limited data available in this study, which covered a period of rather strong inversion (mean air temperature at $z \approx 1.5$ m of $+7.9°$ C), led to the application of the outlined logarithmic approach. Mean values of the main meteorological variables for the two daily intervals are shown in Table I and Figure 3.

The sensible and latent heat gain or loss were calculated for hourly intervals from:

$$Q_H = \frac{P_a C_p}{0.622 R \bar{T}} \frac{k^2 u_1 (T_2 - T_0)}{\ln\left[(z_1+z_0)/z_0\right] \ln\left[(z_2+z_0')/z_0'\right]} \tag{15}$$

$$Q_E = \frac{L_E}{R\bar{T}} \frac{k^2 u_1 (e_2 - e_0)}{\ln\left[(z_1+z_0)/z_0\right] \ln\left[(z_2+z_0')/z_0'\right]} \tag{16}$$

https://doi.org/10.3189/S0022143000032093 Published online by Cambridge University Press

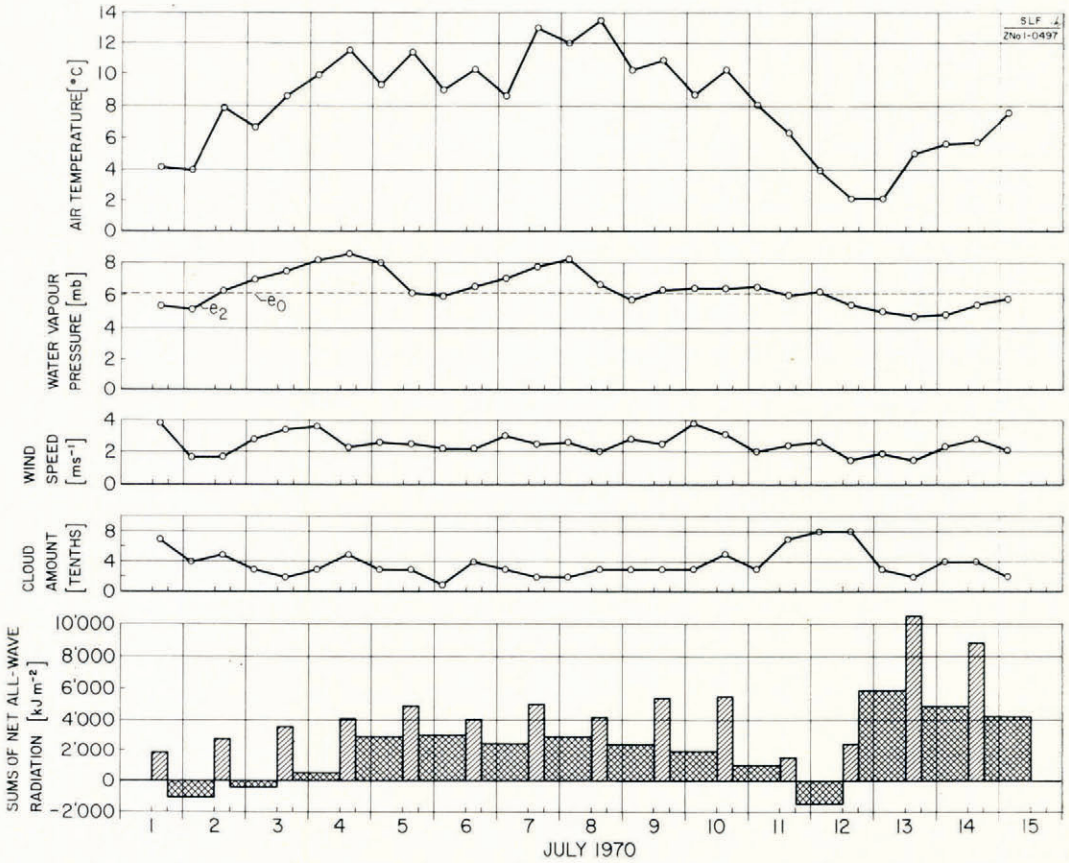

Fig. 3. Mean values of air temperature, relative humidity, wind speed and cloud amount for a 6 h and an 18 h period for successive 24 h intervals. The totals of net all-wave radiation are also represented for the same daily periods.

where P_a denotes the atmospheric pressure (taken as constant: 750 mbar), R the universal gas constant, $\bar{T}$ the mean temperature of the considered air-layer, u_1 and z_1 the wind speed and its height of measurement respectively, T_2 the air temperature and e_2 the water vapour pressure at the height z_2, T_0 and e_0 the temperature and the vapour pressure respectively at the surface, and L_E the latent heat of condensation. Hourly mean values were used for the calculations. A comparison between temperatures recorded at the Rauchfuss meteorological station and those measured in a wooden Stevenson screen and with an aspirated thermometer suggested that the "Rauchfuss" values were too high during day-time and too low during night-time, probably as a result of intensified radiation influences. Therefore, the air temperatures recorded within the metal screen of the Rauchfuss meteorological station had to be slightly corrected. Because the snow-pack studied was melting throughout the observation period ($T_2 \geqslant +0.1^\circ$ C), the snow surface temperature and its vapour pressure were known and assumed equal to T_0 and e_0 respectively. During night-time the partial freezing of the liquid water of the surface layer prevented its cooling by outgoing long-wave radiation and/or evaporation. In a first run the surface roughness length z_0 and the scaling length z_0' were assumed to be equal. The surface roughness parameter z_0 was estimated on the basis of a roughness element description (Lettau, 1969):

$$z_0 = 0.5 h^{\star} s S^{-1} \qquad (17)$$

https://doi.org/10.3189/S0022143000032093 Published online by Cambridge University Press

where h^* is the effective obstacle height, s the silhouette area measured in the vertical crosswind-lateral plane and S the specific area of the obstacles in the basal horizontal plane. According to Lettau this approach is especially feasible for periods with light to moderate winds blowing from the same direction. Under such conditions z_0 is determined by macro-features of the surface rather than by microfeatures of the material. Because the average horizontal wind speed was only 2.5 m s^{-1}, the direction mostly down-glacier, and the nearly level surface of the experimental site consisted of fairly regular sun cups during the first 10 d (Fig. 2), the roughness-element description seemed to be adequate. The average silhouette of the cups could be described by a sinusoidal curve with a wave length of 0.4 m and an average amplitude of 40 mm. Consequently $h^* = 80$ mm, $s = 1.6 \times 10^4$ mm^2, $S = 12.6 \times 10^4$ mm^2 and $z_0 = 5$ mm.

During the last three days, glacier ice was exposed. In the beginning it consisted of smooth superimposed ice, afterwards of old glacier surface ice. Since the previous procedure was no longer applicable, a surface roughness length $z_0 = 0.5$ mm was assumed. This average value was derived from reports of Kutzbach (1961) and Grainger and Lister (1966).

Results and discussion

The melt rates (SM) were calculated for hourly intervals using the heat-balance equation (9), by

$$SM = \frac{Q_{SM}}{L_F} \tag{18}$$

where L_F is the latent heat of fusion. The values obtained were then summed daily over two successive time periods in order to get heat-balance melt rates, which were comparable with the previously mentioned mass-balance melt rates. Table I and Figure 4 show the measured and calculated melt for the first 6 h and the remaining 18 h for every 24 h interval.

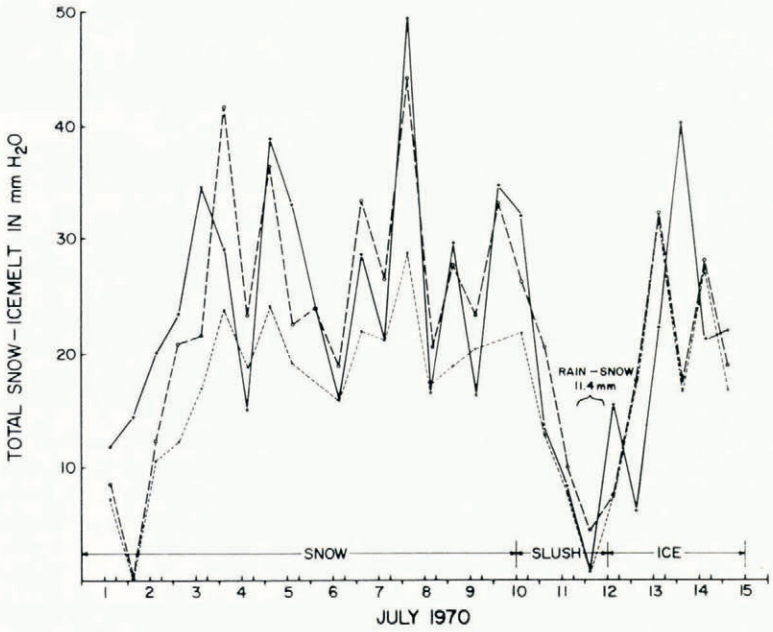

Fig. 4. Calculated and measured melt rates for the first 6 h and the remaining 18 h of a 24 h interval.

+———+ SM_M, *measured melt*
○- - - -○ SM_{C1}, *calculated melt (Run 1)*
●·····● SM_{C2}, *calculated melt (Run 2)*

https://doi.org/10.3189/S0022143000032093 Published online by Cambridge University Press

As mentioned before, no specific distinction between the z_0 and a similar scaling length for the temperature and specific humidity profiles was made in the first calculation run. However, because this parameter has a marked effect on the results and various authors suggested that the assumption $K_M \approx K_H \approx K_E$ was not valid in a very small sublayer at the surface, a separate scaling length z_0' for the temperature and the specific humidity was introduced in a second run. Based on results of Sverdrup (1936), Ambach (1963) and Holmgren (1971) z_0' was chosen two orders of magnitude smaller than z_0.

The observation period covers nine days with continuous snow cover (1 to 10 July) and five days with slush or ice-covered ground. During a single period of overcast (11 to 12 July) a total of 11.6 mm of a mixture of rain and wet snow was recorded. Because this precipitation had no substantial heat content and ran off almost as soon as it was deposited on the surface, there was no need to include it in the heat-balance calculations. The previously mentioned measuring procedures could only be fully applied for the period with snow cover, therefore the following discussion is restricted mainly to these conditions. The values of SM_{M} are measured melt rates, presented as totals for two different consecutive time intervals per day. The values of SM_{C_1} (Run 1) and SM_{C_2} (Run 2) are total values too, computed by means of hourly heat-balance calculations. The difference between SM_{C_1} and SM_{C_2} indicates the magnitude of deviation which can be expected when different roughness parameters are used in the heat-balance calculations; in the first case (SM_{C_1}), only one parameter, z_0, was used, and in the second case (SM_{C_2}), two parameters, z_0 and z_0'. Because the second version underestimates the actually measured melt rate almost consistently, preference is given to the first one. The calculated melt rate (SM_{C_1}) either over or underestimates the measured melt rate, probably depending on the changing atmospheric stratification, which cannot be taken into account with the heat-balance approach outlined. However, a considerable amount of the deviation can be attributed to measurement errors. The maximum relative error for a single measured melt rate was estimated by partial differentiation of Equation (3):

$$\frac{\Delta(SM)}{SM} \leqslant \frac{\Delta\rho_{\mathrm{i}\Delta h}(t_0)\ \Delta h + \Delta(\Delta h)\ \rho_{\mathrm{i}\Delta h}(t_0) + \Delta\rho_{\mathrm{i}\Delta h'}(t_0)\ \Delta h' + \Delta(\Delta h')\ \rho_{\mathrm{i}\Delta h'}(t_0)}{SM} + \\ + \frac{\Delta\rho_{\mathrm{i}\Delta h'}(t_1)\ \Delta h' + \Delta(\Delta h')\ \rho_{\mathrm{i}\Delta h'}(t_1)}{SM} \qquad (19)$$

where $\Delta\rho_{\mathrm{i}} \leqslant \Delta\rho_{\mathrm{s}} + \Delta\rho_{\mathrm{w}}$. Possible errors for the different parameters are as follows:

$$\begin{aligned} \Delta\rho_{\mathrm{s}\Delta h} &= 24\ \mathrm{kg\ m^{-3}} \\ \Delta\rho_{\mathrm{s}\Delta h'} &= 10\ \mathrm{kg\ m^{-3}} \\ \Delta\rho_{\mathrm{w}} &= 0.005\ \mathrm{m^3\ m^{-3}} \\ \Delta h &= 2\ \mathrm{mm} \\ \Delta h' &= 5\ \mathrm{mm} \end{aligned}$$

On the average the maximum error for a 6 h or 18 h melt rate was $\pm 38\%$, whereas for the larger daily melt rates it was $\pm 20\%$. This large error range is mainly due to the considerable error of the snow density measurements. It is caused by electronic drift of the gamma probe, due in part to temperature changes in the detector tube. The various terms, used for calculation of SM_{M} and their absolute errors are tabulated in Table II for two successive periods. Various terms displayed in this table correspond to the snow-profile specifications given in Figure 1. Table II and Figure 1 together illustrate the generally applied measuring and calculation procedure for obtaining the surface and sub-surface melt rate in each time interval. According to Table II the maximum errors of the sub-surface melt rates sometimes unfortunately reach the same order of magnitude as the corresponding measured values thus rendering the measured values questionable for certain periods.

TABLE II. SURFACE AND SUB-SURFACE MELT RATES, INCLUDING THEIR ERRORS, FOR TWO SUCCESSIVE INTERVALS

		Time interval	
Terms	*Units*	*18.00 3 July to 12.00 4 July, 1970*	*12.00 4 July to 18.00 4 July, 1970*
Δh	mm	69	19
$\rho_s \Delta h$	kg m^{-3}	480	579
$\rho_i \Delta h$	kg m^{-3}	461	515
$\rho_w \Delta h$	%	2	6.4
Surface melt	mm	32 ± 2.9	10 ± 1.8
$\Delta h'$	mm	214	212
$\rho_s \Delta h'(t_0)$	kg m^{-3}	485	531
$\rho_i \Delta h'(t_0)$	kg m^{-3}	471	499
$\rho_w \Delta h'(t_0)$	%	1.5	3.2
$\rho_s \Delta h'(t_1)$	kg m^{-3}	537	500
$\rho_i \Delta h'(t_1)$	kg m^{-3}	487	475
$\rho_w \Delta h'(t_1)$	%	5	2.5
Sub-surface melt	mm	-3 ± 4	$+5 \pm 4$
Total melt	mm	29 ± 7	15 ± 6

The maximum or average error for a single calculated melt rate is not known. Because the errors of the many components are unknown and because the errors of the measured values could be large, (cf. maximum errors), the goodness of fit of the two curves in Figure 4 cannot be expressed quantitatively.

Table III displays the various melt and ablation rates for daily intervals and the totals for two longer periods. The comparison of the first two columns (SM_{C1}, SM_{M1}) shows that the

TABLE III. DAILY MELT AND ABLATION RATES AND THEIR TOTALS

	Measurement techniques							
Date	*Melt rate from heat balance*		*Melt rate from surface and sub-surface "ice" densities and surface lowering*	*Melt rate from surface "ice" densities and surface lowering*	*Ablation rate from initial average snow density and surface lowering*	*Ablation rate from total mass loss with cores*	*Ablation rate from total mass loss with snow density profiles*	*Run-off from snow-melt lysimeter*
	SM_{C1} mm	SM_{C2} mm	SM_{M1} mm	SM_{M2} mm	A_3 mm	A_2 mm	A_1 mm	mm
July 1970								
1*	9	(6)	26	14	50	27	46	
2	33	(22)	43	37	38	10	0	
3	63	(41)	63	59	60	1	47	
4	60	(43)	54	34	30	54	15	40
5	47	(37)	57	35	33	84	73	28
6	52	(38)	44	39	37	44	40	35
7	71	(50)	71	64	62	57	72	78
8	48	(36)	46	36	34	45		47
9	56	(42)	51	42	42	49		36
Totals	439	(315)	455	360	386	371		
10	47	(35)	45†		46	45		
11	15	(8)	9		10	9		
12	25	(25)	22		22	22		
13	50	(48)	63		63	63		
14	47	(44)	43		44	43		
Totals	623	(475)	637		571	554		

* The values presented for a certain day j are actually the values calculated or measured from 12.00 h of day j to day 12.00 h of day $j+1$.

† For the period when the surface consisted of slush or ice no sub-surface ice densities could be obtained, thus the values of column SM_{M1} are assumed to be identical with the ones from column A_2.

https://doi.org/10.3189/S0022143000032093 Published online by Cambridge University Press

agreement between the daily totals is closer than it was between the 6 h and 18 h values mentioned above, probably due to error compensation. Consequently, the totals for the 9 d and 14 d periods agree to within a few per cent. As a measure of the agreement the calculated daily values are plotted against the measured values in Figure 5. The solid line represents the line of equivalence and the dashed line the regression line (SM_{C1} on SM_{M1}).

This presentation should be regarded as a visualization of the scattering of the values around the line of equivalence and not as an error evaluation in a strict sense, because abscissa and ordinate values are both subject to errors. However, the small standard error of estimate ($S_{yx} = 7.1$ mm d^{-1}) and the plotted maximum errors for the measured melt indicate that the agreement between the values is satisfactory.

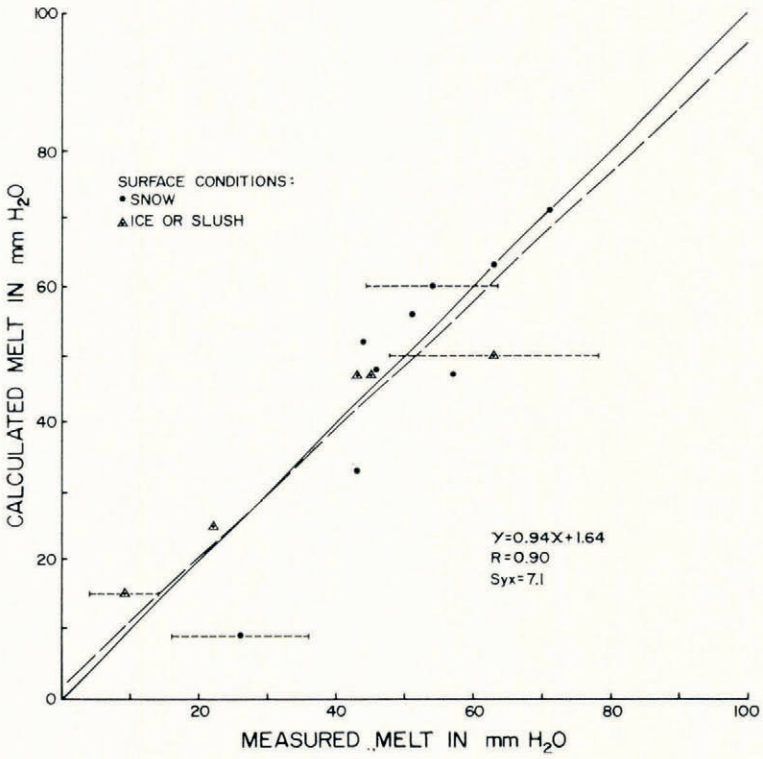

Fig. 5. Calculated daily melt versus measured melt. The range of maximum error for several measured values is shown by a horizontal dashed line. The solid line represents the line of equivalence and the dashed line the regression line.

The fact that a simple heat-balance approach has a certain potential in describing the single heat exchange processes at the snow surface is demonstrated in Figure 6. It shows the calculated and the measured net vapour fluxes, the latter derived by successive pan measurements. The transfer of mass and energy toward the snow surface is taken as positive. The heat-balance calculations favour a slightly higher net gain of mass than the direct measurements, but the direction and the order of magnitude of the fluxes agree roughly. The pan measurements were not carried out during a period of overcast, drizzle and a mixture of snow and rain (10 to 13 July).

The larger differences during the last two days can be explained by the measuring procedure. At the reference location in the plot, the glacier ice was exposed. Consequently, the heat-balance calculations for this period were performed for ice-covered ground ($z_0 = 0.5$

mm), while the evaporation measurements were still executed with snow-filled pans, placed in nearby snow patches. Thus the snow-filled pans, subject to rougher surface conditions, showed larger evaporation rates. The totals for the first 9 d were:

measured net-vapour flux (mass balance): +1 mm of water,
calculated net-vapour flux (heat balance): +3.7 mm of water.

This calculation has been executed using z_0 as sole roughness parameter. During the prevailing fair-weather conditions, the mass balance of the snow-pack was affected by evaporation or condensation processes to a small extent only, although the condensation process supplied 11% of the total absorbed energy, due to its high latent heat.

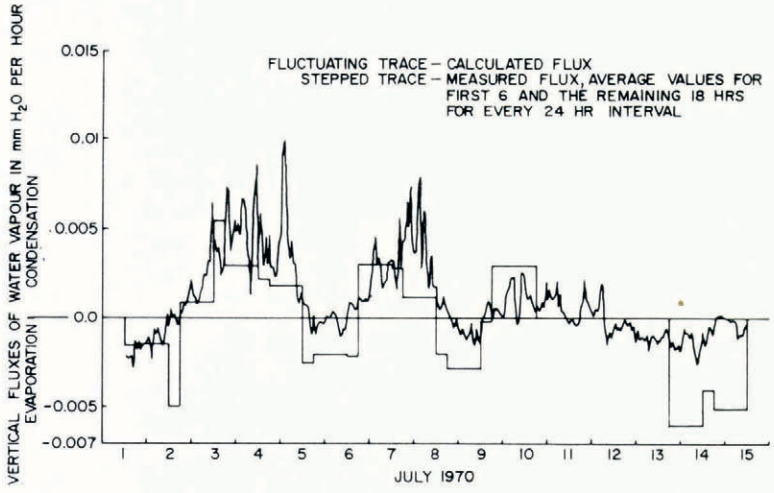

Fig. 6. Calculated and measured hourly vapour flux. Step function is obtained from pan measurements.

When comparing the various ablation rates in Table III, large differences are apparent for certain days. These are caused by water storage effects in the lower part of the snow-pack and by sampling errors (e.g. partial loss of liquid water from sample cores). At the base of the snow-pack a fluctuating water table of 10 to 50 mm was present throughout the first 9 d. Sometimes, lateral inflow of water could apparently make up for the actual mass loss on the upper end of the snow-pack. For such conditions, measured daily ablation rates are not comparable with measured or computed melt rates.

Conclusions

Daily melt rates can be determined with a maximum relative error of 20% by evaluating the ice matrix density (in contrast to the total snow density) of the immediate surface and sub-surface layers and by evaluating the decrease in volume. Neglecting the ice-density changes in the sub-surface layer would, on the average, reduce the daily melt rates by 22%. With heavy melt conditions and more precise instrumentation, e.g. a non-drifting, automatically scanning gamma probe, the method could be used even for shorter intervals, i.e. several hours, where all other methods may be subject to large errors due to the delay in liquid water outflow from the snow-pack. Thus, for short intervals, this method alone provides an opportunity to balance detailed heat-balance equations with a mass-balance quantity to sufficient accuracy.

A small but possible effect of the compaction of the whole snow-pack on the results was not taken into account.

The heat-balance approach gave satisfactory results on a daily basis and a close agreement for longer periods. The distribution of the total absorbed energy between the different components for the whole period was as follows: all-wave net radiation 44%, sensible heat 48%, and the latent heat (condensation) 8%. Wendler and Streten (1969) observed a similar distribution, with the radiative and sensible heat terms interchanged, on an Alaskan glacier in August 1968. This distribution corresponds to the known pattern, often encountered over snow surfaces at low elevations in mid-summer when the convective heat is equal or even exceeds the radiative heat, whereas the condensation process is a rather minor heat source.

It appears that the heat-balance approach described represents a useful method for obtaining melt rates for periods of several days. Applying such an approach, one can avoid the use of a "lumped" melt index like the degree-day factor, and preserve the more physical treatment inherent in heat-balance calculations.

Acknowledgements

This study was supported by grants from the National Research Council of Canada and the Department of the Environment, Inland Waters Branch, Hydrologic Sciences Division, Ottawa, Ontario. I am indebted to Dr O. H. Løken, Head of the Glaciology Subdivision, Hydrologic Sciences Division, Inland Waters Branch, for support in all the aspects of this study. Thanks are also due to Dr F. Morton and Dr A. D. Stanley for their helpful suggestions made during the preparation of this paper.

MS. received 26 May 1972 and in revised form 4 October 1972

REFERENCES

Ambach, W. 1963. Untersuchungen zum Energieumsatz in der Ablationszone des grönländischen Inlandeises (Camp IV-EGIG, 69° 40′ 05″ N, 49° 37′ 58″ W). *Meddelelser om Grønland*, Bd. 174, Nr. 4.

Ambach, W., *and* Hoinkes, H. C. 1963. The heat balance of an Alpine snowfield (Kesselwandferner, 3240 m., Ötztal Alps, August 11–Sept. 8, 1958). Preliminary communication. *Union Géodésique et Géophysique Internationale. Association Internationale d'Hydrologie Scientifique. Assemblée générale de Berkeley, 19–8—31–8 1963. Commission des Neiges et des Glaces*, p. 24–36.

Brunt, D. 1952. *Physical and dynamical meteorology. Second edition, reprinted.* Cambridge, University Press.

Grainger, M. E., *and* Lister, H. 1966. Wind speed, stability and eddy viscosity over melting ice surfaces. *Journal of Glaciology*, Vol. 6, No. 43, p. 101–27.

Haugen, D. A., *and others*. 1971. An experimental study of Reynolds stress and heat flux in the atmospheric surface layer, by D. A. Haugen, J. C. Kaimal and E. F. Bradley. *Quarterly Journal of the Royal Meteorological Society*, Vol. 97, No. 412, p. 168–80.

Holmgren, B. 1971. Climate and energy exchange on a sub-polar ice cap in summer. Arctic Institute of North America Devon Island Expedition, 1961–1963. Part D. *Meddelanden från Uppsala Universitets Meteorologiska Institution*, Nr. 110.

Hubley, R. C. 1954. The problem of short period measurements of snow ablation. *Journal of Glaciology*, Vol. 2, No. 16, p. 437–40.

[International Hydrological Decade.] 1970. *Combined heat, ice and water balances at selected glacier basins: a guide for compilation and assemblage of data for glacier mass balance measurements.* Paris, UNESCO/IASH. (Technical Papers in Hydrology, 5.)

Kutzbach, J. 1961. Investigations of the modification of wind profiles by artificially controlled surface roughness. *Annual Report, Department of Meteorology, University of Wisconsin, Madison*, 1961, p. 71–113.

LaChapelle, E. R. 1959. Errors in ablation measurements from settlement and sub-surface melting. *Journal of Glaciology*, Vol. 3, No. 26, p. 458–67.

Lettau, H. 1969. Note on aerodynamic roughness—parameter estimation on the basis of roughness—element description. *Journal of Applied Meteorology*, Vol. 8, No. 5, p. 828–32.

Mellor, M. 1964. Properties of snow. U.S. Cold Regions Research and Engineering Laboratory. *Cold regions science and engineering*. Hanover, N.H., Pt. III, Sect. A1.

Miller, D. H. 1950. Albedo of the snow surface with reference to its age. *Civil Works Investigations. Technical Bulletin* No. 6.

Müller, F. [1969]. Automatic climatological recording stations in remote areas. (*In Canada. National Research Council. Associate Committee on Geodesy and Geophysics. Subcommittee on Hydrology. Proceedings of Hydrology Symposium No. 7, Victoria, British Columbia, 14 and 15 May 1969.* [Ottawa], Inland Waters Branch, Dept. of Energy, Mines and Resources, for the Subcommittee on Hydrology, p. 205–17.)

Müller, F., *and* Keeler, C. M. 1969. Errors in short-term ablation measurements on melting ice surfaces. *Journal of Glaciology*, Vol. 8, No. 52, p. 91–105.

Radok, U., *and others*. 1961. On the calorimetric determination of snow quality, [by] U. Radok, S. K. Stephens and K. L. Sutherland. *Union Géodésique et Géophysique Internationale. Association Internationale d'Hydrologie Scientifique. Assemblée générale de Helsinki, 25–7—6–8 1960. Commission des Neiges et Glaces*, p. 132–35.

Smith, J. L., *and others*. 1966. *Portable radioactive isotope snow gages for profiling snowpacks, by J. L. Smith, D. W. Willen, M. S. Owens*. [Oak Ridge, Tennessee], U.S. Atomic Energy Commission. Division of Technical Information. (TID 23368.)

Sumner, C. J. 1965. A long-period recorder for wind speed and direction. *Quarterly Journal of the Royal Meteorological Society*, Vol. 91, No. 389, p. 364–67.

Sverdrup, H. U. 1936. The eddy conductivity of the air over a smooth snowfield. Results of the Norwegian–Swedish Spitsbergen Expedition in 1934. *Geofysiske Publikasjoner*, Vol. 11, No. 7, p. 5–49.

Wendler, G., *and* Streten, N. A. 1969. A short-term heat balance study on a Coast Range glacier. *Pure and Applied Geophysics*, Vol. 77, No. 6, p. 68–77.

APPENDIX

Description of instruments

Net radiometer: Thornthwaite net radiometer which is similar to the Funk radiometer but is not as sensitive. It measures directly the radiation balance (short- and long-wave components together). Both faces of the sensor are shielded with polyethylene hemispheres, which are kept inflated with dry air, flowing through silica gel. The calibration certificate for the whole range was issued by the manufacturers.

Meteorological station: Australian made station (Rauchfuss—C.S.I.R.O.) recording air temperature and relative humidity at the level of 1.5 ± 0.2 m and wind speed and direction at the standard level of 2 ± 0.2 m. The level of sensors above snow or ice surface changed slightly during the observation period due to the surface lowering. In order to keep the changes within the above-mentioned limits the station was adjusted every second or third day. The level changes were taken into account in the calculations.

For long-term performance of these stations cf. Müller (1969) and for design details of the wind system and the recorders cf. Sumner (1965).

Ablatometer: Own make. It consisted of two vertical posts, positioned parallel and 2 m apart in the snow cover and driven with their lower ends into the glacier ice. The upper ends of these posts were connected horizontally with a thin wooden bar, which was 0.5 m above the snow surface at the beginning of the observation period. The lower edge of this bar was used as reference height from which the lowering of the snow surface was measured by a measuring stick at 0.1 m intervals along the bar.

Gamma transmission probe: The system utilized is a two-probe radioactive snow gauge, commercially available from Troxler Electronic Laboratories, Raleigh, North Carolina, U.S.A. It includes a ^{137}Cs-source (5 mCi), a scintillation detector (NaI thallium activated crystal), a pulse-height analyser and a scaler. Detector, analyser and scaler are referred to as the SC-10 Density System. For detailed description cf. Smith and others (1966).

Pyranograph: A Robitzsch bimetallic pyranograph, measuring the total short-wave radiation from sun and sky. Trade name: Belfort pyrheliograph (Belfort Instrument Company, Baltimore, Maryland, U.S.A.).

Precipitation gauge: Standard gauge of the Meteorological Service of Canada, consisting of a cylindrical container of 5 inches (127 mm) diameter. This gauge was attached to a vertical post in such a way, that the orifice could always be positioned 0.5 m above surface. The amount of precipitation was determined by measuring the volume of water with a graduated glass cylinder.

Evaporation pans, snow-melt lysimeter and calorimeter: Own make. Because in this case the measuring procedures are inherent parts of this study, these instruments and the measuring procedures are described in the corresponding sections of the paper.